

# Directionality, Fractals and Chaos in Wind-shaped Forests

*Alexander Robertson*

## **ABSTRACT**

Within the last decade three new statistical paradigms have emerged for analysing directional variates and modelling non-linear dynamical systems—circular statistics, fractal geometry and chaos theory. Although the directional effects of wind on agricultural crops and trees have been described from ancient times, it has mainly been within the last two decades that formal statistical tests of directionality, known as circular and spherical statistics, have been developed. Circular and spherical statistics have been applied in biology and geostatistics but rarely in biometeorology. Similarly, the time-honoured Euclidean geometry, based on the idealized simplicity of homogeneity and symmetry, have prevailed. Euclidean geometry is inadequate for describing the geometry of many objects, particularly the myriad of scaling factors, lacunarity and heterogeneity of agricultural crops, trees and forests. To deal with these problems the notion of fractal geometry—the calculus of heterogeneity—was introduced. Mathematics and statistical theory are rooted in the belief that physical systems can potentially be described and predicted. However, the new paradigm of chaos theory clearly shows that this is not the case for most, if not all, non-linear phenomena. Undoubtedly, the interaction between wind and forests is a non-linear system within which, to use a well-worn cliché, short-term prediction is possible whereas long-term prediction is not. This paper provides a brief overview of the application of these new paradigms to the study of wind effects on forests, drawing mainly on exploratory work conducted on the wave forest phenomena in Newfoundland.

## **I. INTRODUCTION**

In many parts of the world, the impact of wind on forests is obvious. Hurricanes (typhoons) destroy forests in Japan, Mauritius and eastern North America. Gales cause wind throw in young plantations in northern Europe, in aspen stands in northern Caucasia and Bavaria, and in *Shorea* stands in Sarawak. Windiness is responsible for the poor form of Norway spruce in parts of Poland, Scots pine in northern Sweden and black spruce at the tree line in northern Canada. Wind has a considerable influence on the population dynamics of subalpine spruce—fir forests in the Adirondack Mountains. It creates niches for Sitka spruce in the coastal forest of western North America. It is also responsible for the absence of beech in natural forests of the Puszlave valley in Poland and the treeless tundra on the mountains of eastern Siberia. There are many peculiar examples of wind-shaped forests, such as the strong curvature of ‘copse and spinney’ in the UK and the standing dead tree strips of peculiar fir wave forests in coastal forests of Newfoundland, and subalpine forest in Japan and the northeastern USA.

Wind data are incorporated into models of carbon balance, nutrient cycling, surface energy balance (evapotranspiration, turbulent transfer), paedogenesis, biodiversity, biomass productivity and longevity. Also, wind creates patterns in forests that provide proxy evidence of short- and long-term climatic changes including changes in winter climate, and palaeowinds (Scott et al., 1988; Allen, 1992; Robertson, 1992).

Intuitively, we sense that wind turbulence is a patterned instability with well-defined regions and states. Technically, however, wind flow over forested terrain is difficult to quantify. Across the Boreal Biome, wind data from standard meteorological networks are scarce and short term, and are usually collected in treeless sites and restricted to average hourly, daily or longer time-scales. This type of climate-scale database is of limited use to forest meteorology at smaller scales mainly because it precludes the principal features of wind regimes at weather time-scales, namely, high wind speeds of short duration (less than 1 h) that have as much influence on forest dynamics as average wind speeds. Consequently, forest ecodynamic models that use such a climate-scale wind database are more or less limited to steady-state dynamics and unable to deal with transient dynamics.

Another statistical reason for the difficulty in incorporating transient dynamics into forest ecodynamic models is that conventional (linear) statistics cannot account for scaling factors in non-linear deterministic processes, such as the invariance (self-similarity) of the probability distributions under space—time rescaling. In fact, the quantification of interscaling relationships remain among the critical and unsolved problems that play a key role in understanding land—atmosphere interactions (Wood and Lakshmi, 1993).

At the other extreme, there have been considerable advances in modelling the complexity of surface wind flow in hilly terrain, flow over and within forests, and ecophysiological responses to wind at short time-scales. However, there is no model that adequately describes and deals with wind—forest interactions—except in the crudest terms.

Within the last decade new statistical paradigms have emerged which improve understanding of interscale relationships of forest—atmosphere interactions. Among them are circular statistics for analysing directional phenomena, fractal geometry for modelling effects of wind on forest structure, and chaos theory for modelling non-linear dynamical systems.

Directional phenomena in nature have been described from the earliest civilizations. The modern concepts of circular statistics date back to Florence Nightingale's 'coxcomb' graphical displays of "preventable and mitigable zymotic diseases" reproduced by Fisher (1993). However, most of the formal statistical tests of directionality (circular statistics) have emerged only within the last two decades. Indeed, only three books devoted entirely to circular statistics have been published to date (Mardia, 1972; Batschelet, 1981; Fisher, 1993), plus a couple of extensive chapters (Zar, 1974; Upton and Fingleton, 1989). Furthermore, circular statistical algorithms have not yet been incorporated into widely used statistical computer software packages. Therefore, it is not surprising that circular statistics lies outside the purview of mainstream science.

By contrast, the combination of fractal geometry and chaos theory is advancing rapidly, with new books on the subject appearing weekly. In addition, there are hundreds of multidisciplinary journal papers published monthly. There is also a wide range of PC-based computer software for fractal design and chaos analysis available for all skill levels. This paper discusses the potential of circular statistics, and the new science of fractals and chaos for quantifying forest—wind interactions. Applications of circular statistics, fractals and chaos are drawn mainly from examples of unique wind-shaped forests in Newfoundland.

## **2. CIRCULAR STATISTICS: THE CALCULUS OF DIRECTIONALITY**

Flagged trees, streamlined forest canopies, dieback along the forest edge, and strips or patches of wind throw are common features of forested landscapes in windy climates. Intuitively, these distinctive features have provided a visual estimate of the prevailing surface wind flow over the landscape since ancient times. But only since the 1970s have quasi-empirical models been available which estimate wind speed and wind direction from the degree of tree flagging (Wade and Hewson, 1979; Yoshino, 1988). In

relation to predicting the influence of wind flow on the spread of forest fires, Sceicz et al. (1979) developed a model with various parameters of stand density, crown projection area, shrub layer and large boulders for remote sensing of 'real-time' wind flow in open-growing black spruce—lichen forest in Labrador.

The windiness of a region, at least from directions which affect forests the most, can be estimated from the surface profile of forest canopies. For example, a smooth, close-knit canopy indicates strong persistent wind, whereas a very rough forest canopy indicates low wind speeds.

From a forestry and agrometeorology perspective, these simple models are not simply rough estimates of surface wind flow; they encapsulate the sum of biometeorological influences at both weather and climatological time-scales. Therefore, they provide a useful starting point for more elaborate and specialized meteorological studies.

Misinterpretations can arise when using trees as biological indicators of wind flow if certain biophysical factors are not considered. First, evergreen and deciduous trees respond differently to the seasonality of winds at weather and climate timescales. In Newfoundland, for example, the direction of crown deformation of larch (*Larix*)—a deciduous conifer—and birch (*Betula*) tend to be controlled by the less frequent strong summer westerlies rather than the persistent and usually benign 'prevailing' southwesterlies. Conversely, cold, dry northeasterly winter winds cause most of the flagging of evergreens, such as spruce (*Picea*) and fir (*Abies*) along the north coast.

In northern coastal areas, freezing rain also causes tree deformation, more so in evergreens than deciduous trees. However, experienced observers can distinguish between deformation by wind and freezing rain, respectively, insofar as the latter usually results in coniferous trees with multiple, contorted boles and deciduous trees (other than larch) with many of their branches broken or stripped off.

Differential radiation balance can also cause extreme flagging of trees that can be mistaken for wind-flagging. At Hallormstadir in east Iceland, noted for its low average wind speed and high percentage of calms, open-growing tree forms are symmetrical with the exception of the strong flagging of a patch of 30 or so young Colorado blue spruce (*Picea pungens*) oriented towards the south-southeast. S. Blondal (personal communication 1993) observed that, during spring, solar radiation from a low sun angle is sufficient to maintain temperatures above the freezing threshold which permits shoot survival on the southerly aspects of the crown, whereas temperatures fall well below the freezing threshold to kill new shoots on the shaded north side of crowns. Undoubtedly, flagging by differential radiation balance is a common though rarely reported phenomenon at high latitudes.

Generally, wind speeds greater than 7 m s<sup>-1</sup> occurring over several days and weeks are required to cause noticeable tree deformation (flagging). Therefore, when calibrating tree deformation indices it is more appropriate to analyse wind data using statistics of extremes, such as the technique developed by Gumbel (1958), the father of statistics of extremes, for a wide range of disciplines and adapted for ecology by Gaines and Denny (1993).

## **2.1. Directionality**

The earliest classifications of wind directions are the eight winds of ancient Greek mythology. The eight winds are portrayed in reliefs on the Tower of the Winds in Athens, built in the first century BC by the astronomer Andronikos of Kyrros, hence its correct name 'Horologium of Andronikos Kyrrestes'. Centuries of erosion have obscured the details in the reliefs. However, replicas of the reliefs can be seen on the magnificent Tower of Winds built in Oxford between 1772 and 1776. The Oxford 'copy' (considerably larger than the original) is perched upon the Radcliffe Observatory and is a conspicuous landmark and the focal point of Green College (Fig. 1). Incidentally, the Radcliffe Observatory also

happens to be among the sites that contributed to Oxford having one of the longest continuous instrumental meteorological records in the world.

The octagonal faces of the Tower of Winds in both Athens and Oxford are appropriately aligned to coincide with the direction from which the eight winds in Greek mythology blow. The reliefs of each wind at the top of the octagon are as follows:

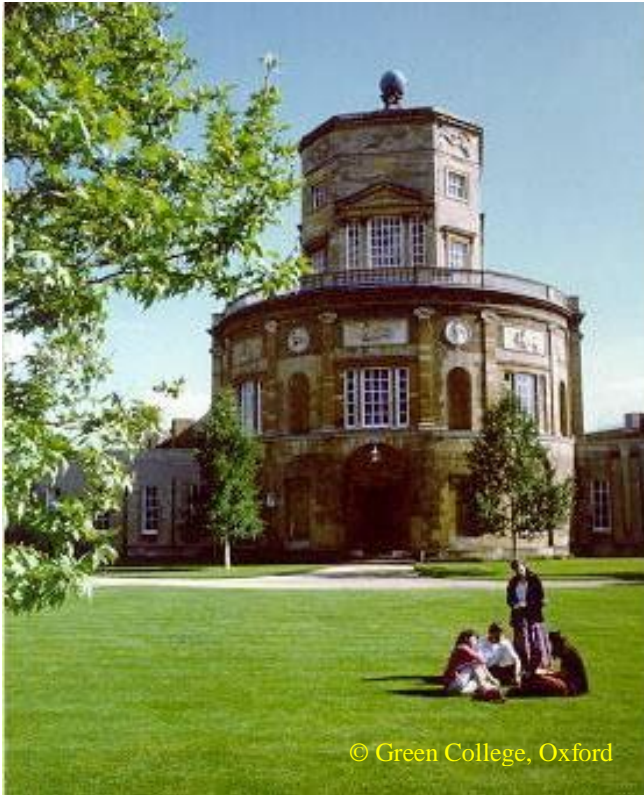


**Fig. 1. The Tower of Winds, Green College, Oxford. Reliefs of the eight winds of Greek mythology are located at the top of the octagonal section of this ~copy' of the ancient Tower of Winds in Athens.**

**North Wind, Boreas**, wears a thick-sleeved cloak with folds blowing in the air, and high-laced buskins, and is blowing a twisted shell;

**Northeast Wind, Kaikias**, empties a shell full of hailstones;

**East Wind, Apeliotes**, displays flowers and fruit;  
**Southeast Wind, Euros**, with his right arm muffled in a cloak, threatens high winds;

**South Wind, Notos**, empties a shower from his urn;

**Southwest Wind, Lips**, drives a ship before his gale;

**West Wind, Zephyros**, bodes showers;

**Northwest Wind, Skiron**, bears a bronze vessel with which he dries up the rivers.

The impact of the winds from eight directions on animal and plant husbandry including arboriculture was described by Theophrastus of Eresos (370—285 BC) in his book *De Ventis*.

## 2.2. *Analysing directional data*

Indexing a golf course provides an interesting example of how biotic and abiotic factors are integrated to achieve a specific directional result. It involves setting a score standard (par) based on a strokes index set for each hole on the golf course. Usually, par score for each hole is based on the score which a top-class player would be expected to have at a particular hole. By analogy, the probability of a seed or insect (golfer) reaching its target and competing successfully for resources with the least effort (obtaining the lowest score among competitors) depends on the fitness of the biota (handicap)—taking into account environmental constraints (difficulty of the terrain, obstacles and weather), especially wind speed and wind direction.

Muirheartaigh and Sheil (1983) based their approach to indexing a golf course on the proportion of players who equalled or bettered par for the course, rather than concentrating on the best players. Their model involved fitting a logistic function to the data for each hole and determined the probability,  $P_i$  of par for the course by calculating the joint distribution of variables

$$P_i = \sum_{H=1}^2 \frac{1}{2} \iint g_i(w_s, w_d, H) f(w_s, w_d) dW_s dW_d$$

where  $W_s$  and  $W_d$  are wind speed and direction, respectively;  $H$  is the golfer's handicap, and  $f(w_s, w_d)$  is the joint distribution function of wind speed and wind direction. Muircheartaigh and Sheil used the offset normal distribution (Mardia, 1972) to calculate the joint probability distribution function (p.d.f.) of wind speed and wind direction. The distribution of the independent variables is evaluated to establish the degree of difficulty and the appropriate ranking of par for the entire course. Strictly speaking, the directional data required for indexing a golf course are implicit only in the structure of wind direction.

For explicit directional data, Fisher and Powell (1989) posed the following questions germane to circular statistics:

- (1) Is a given set of measurements isotropic, or is there evidence of a preferred direction?
- (2) If there is a preferred direction, what is a suitable estimate of it, and what error can be associated with this estimate?
- (3) Given two sets (or more) of samples of data, do they come from populations with the same preferred directions?
- (4) If two or more samples have a common underlying preferred direction, how should the separate information be pooled to produce an appropriate answer?

Regarding the first two questions, Fig. 2 illustrates the basic circular statistics for a unimodal distribution (i.e. directionality having a single critical value).

Robertson (1987) posed similar questions concerning the directionality of forest dynamics within a wave forest. He showed the effectiveness of circular statistics for profiling the transition from biotic (competition) processes causing crown asymmetry to abiotic (mainly wind) processes as the dominant cause of crown asymmetry.

Similarly, the curvature of two isolated birch stands on a lava field in south Iceland is a response to winds from two directions that evoke an entirely different response. Preliminary analysis of directional data, namely the distribution of regeneration and height of birch, suggests that the curved outline of the stand, which rises towards the east, results from the spreading of seed by dry northeasterlies in winter; whereas the curve rising from the south is caused by the stress of persistent southerly winds (7-11 m s<sup>-1</sup>) on the foliage (A. Robertson and A. Aradottir, unpublished data, 1993).

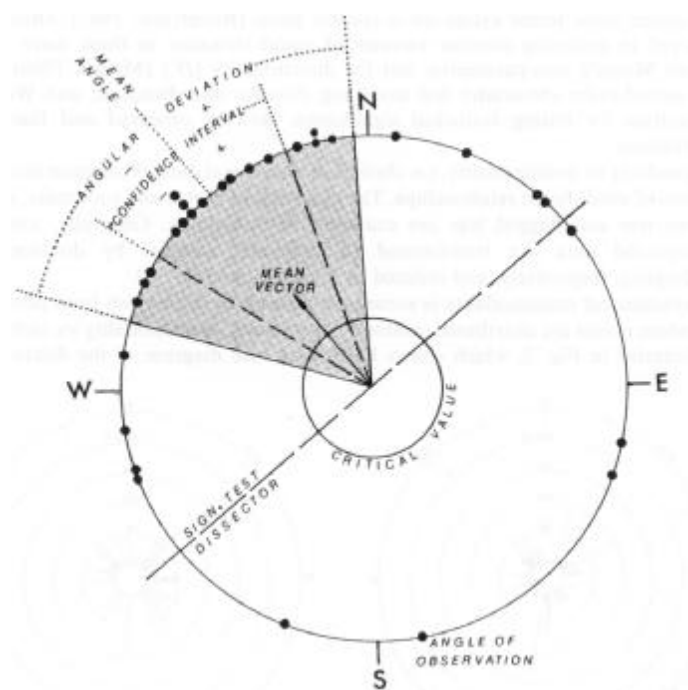


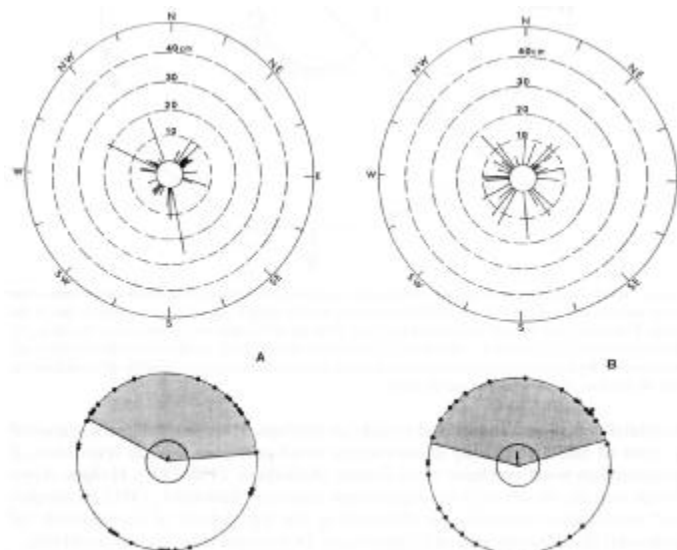
**Fig. 2.** Graph illustrating basic circular statistics for unimodal distributions. The points on the edge of the circle are circular variates. The tip of the mean vector,  $r$ , may range from zero at the centre to one on the circle. The inner circle bounds the critical value,  $r(c\sim)$ . If the tip of the mean vector lies outside this circle, the directionality is significant at  $P = 0.05$  level of significance. Alternatively, significance of directionality can be estimated by a dissecting line perpendicular to the mean vector—the lower the number of variates on one side of the line, the more directional the data.

Among the earliest and most practical bivariate tests for directionality is the Hotelling confidence ellipse (Hotelling, 1931). It includes elliptical analogues for standard deviation, variance and confidence intervals. Hotelling's ellipse was applied to tests of the directionality of asymmetric wood properties such as orientation of compression wood and basic wood density (Robertson, 1990, 1991). Hodges—Ajnes V-test and the Batschelet's significance test dissector (Batschelet, 1981) are simpler and more direct methods for determining the significance of directionality of unimodal distributions around a single mean. Two sample tests, such as the Mardia-Watson-Wheeler test and Mardia's uniform test score (Mardia and Spurr, 1973), are convenient statistical techniques for checking the directional similarity between a pair of unimodal distributions. For example, the Mardia-Watson-Wheeler test was used to test the consistency of surface wind flow patterns in mountainous terrain over several days (Zak and Minnich, 1991). Similarly, Mardia's uniform test score was used to test the directional similarity of crown deformation within a series of three contiguous wave forest cycles on a coastal plain (Robertson, 1987). Other tests deployed in analysing circular variates of stand structure in these wave forests include Moore's non-parametric test for directionality ( $D^*$ ) (Moore, 1980) which is a second-order (bivariate) test involving distance and direction; and Watson's  $U^2$  statistic for testing statistical significance between observed and theoretical distributions.

Bimodality or multimodality, i.e. clusters of directional data, is common in circular variates of wind—forest relationships. The main axis of crown and root mass, a wind-thrown tree and flagged tree are examples of bimodality. Generally, axial and quadrimodal data are transformed to unimodal samples by doubling and quadrupling, respectively, and reduced to multiples modulo 360.

Asymmetrical multimodality is sometimes difficult to distinguish from isotropism (i.e. where points are distributed randomly on a circle). Multimodality vs. isotropism is illustrated in Fig. 3, which shows both (1) a rose diagram of the distance and direction from a point representing a tree location to the centroid (centre of mass) of the Thiessen polygon within which the point occurs and (2) the corresponding circular statistics diagram (statcircle). Under assumptions of unimodality, the distribution shown in Fig. 3(a) would be isotropic (non-directional), although it clearly exhibits three distinctive clusters. By comparison, the distribution in Fig. 3(b) is closer to the definition of isotropic. Apparently, there is no formal circular statistical test powerful enough to distinguish between these distributions. The graphs are part of a series that reflect a distinctive phase change from a clustered spatial point pattern (owing to biotic (competitive) processes) in the early stage of stand growth to a random pattern (Poisson forest). This is due primarily to effects of wind in the mature stage of stand development (Robertson, 1993a).

**Fig. 3. Two circular distributions representing the direction and distance from a tree location to the centre of mass of its Thiessen (Dirichlet) polygon (top) and their circular statistics graph (below). Treated as unimodal distributions, directionality is not significant (i.e. the mean vector lies within the critical radius at  $P$  0.05 level of significance). However, one statcircle (bottom left) clearly shows three distinctive directional clusters, whereas the other is essentially isotropic. These illustrate that a multimodal test in either case would be more appropriate.**



The unimodal directional model is very useful for predicting events restricted to a narrow range of angles, such as the alignment of tree branches and boles snapped off by wind, wind throw, and deformation by wind or differential radiation. However, such a model is not valid for studying the effects of wind on the planar directionality of seed and insect dispersal, the spread of forest patches or expansion of gaps, growth or decline of root mass or crown area, or changes in biodiversity, all of which have multiple ‘targets’ or lateral dispersions with a wide circular variability and multimodal or isotropic distributions.

### ***2.3. Circular regression***

Recent innovations in circular regression techniques have many advantages over the standard linear regression format for testing associations between circular variates. The usual way to approach the problem is to transform angular data into linear equivalents, treat them as independent variables and analyse them using standard linear statistical models. In doing so, however, the statistics tend to obscure the essence of directionality of circular correlations. Alternatively, we could use techniques such as Mardia’s rank correlation procedure (Mardia, 1975) to test uniformity between the directional populations. This is a non-parametric measure of circular correlation in which Mardia’s test statistic,  $M^*$ , is analogous to Kendall’s  $r_K$  statistic. Similarly, the Jupp-Mardia correlation coefficient (Jupp and Mardia, 1980) is a parametric test that requires only a short BASIC algorithm provided by Upton and Fingleton (1989). The test statistic  $r_{J\_M2}$ , ranging from zero to one, is the circular regression analogy of Pearson’s  $r^2$  statistic of linear statistics.

In addition to these general approaches, Nicholas Fisher, a major contributor to the development of circular (and spherical) statistics, reflected the state of the art in his most recent book (Fisher, 1993). His book features new developments in nonparametric smoothing, bootstrap-based techniques, and appropriate methods for exploratory analysis and graphical display (and, notably, pitfalls to avoid when constructing rose diagrams).

### ***2.4. Spherical statistics***

Spherical statistics is used mainly in geostatistics, notably the spherical distribution of magnetic fields in the Earth’s crust (Fisher et al., 1987). Spherical statistical models, like circular models, are limited to point processes on a convex hull (a smooth surface). Similarly, for convenience, biomechanical models of wind—tree relationship define the geometry of a bole, crown shape and root plate as an invariant convex hull. This is a practical approach for many circumstances because it allows us to assess the impact of wind on the spherical directionality of asymmetry and heterogeneity of root mass, bole form, wood density, branch patterns, wood properties, leaf area, photosynthetic efficiency, respiration, transpiration, stomatal conductance, biochemical translocation, etc. Essentially, one would envelop a three-dimensional image (e.g. tree crown) with a sphere and project the direction of its vector (or vectors) as a point (or points) on the sphere. Spherical statistics also contains algorithms for calculating the mean vector (centre of location) of points distributed over the entire sphere or part of the sphere.

Generally, in areas with a low average wind speed, the geometry of widely spaced trees is quasi-symmetrical. This means that vectors of spherical variates within the tree, such as leaf area index, photosynthetic efficiency and branch mass, produce a random point pattern on a sphere. By contrast, the geometry of trees growing in windy conditions or within closed canopies with contiguous crowns is asymmetric; hence, vectors tend to be concentrated within a spherical wedge and, therefore, produce a clustered point pattern on the sphere. Also, spherical variates may be restricted to equatorial, great circle or bipolar distributions.

Fisher et al. (1987) and Upton and Fingleton (1989) gave extensive discussions on the formulation and relative merits of these and other spherical distributions. Table 1 provides a brief list of the spherical distributions.

### 3. FRACTAL GEOMETRY: THE CALCULUS OF HETEROGENEITY

Fractal geometry is a new language; “*once you speak it, you can describe the shape of a cloud as precisely as an architect can describe a house*” (Barnsley, 1989). Milne (1991) called it ‘~the calculus of heterogeneity’. Peitgen et al. (1992) provided an extensive introduction to the methods of fractal geometry. In everyday experience, we observe that, in Euclidean measure, the length of a piece of string has one dimension, a sheet of paper two dimensions and a box three dimensions. However, often we sense that it is not always clear which dimension should be assigned. A string, for example, is more than a line and less than a plane, but has a two-dimensional *form*. In other words, it has a ‘fractional’ dimension that lies between the classical one and two dimensions. What has happened here is that Euclidean geometry fails us by not providing a measure of this fractional dimension. The concept of fractal geometry evolved to resolve problems of this nature. Mandelbrot (1983) created the term ‘fractal’ from the Greek adjective ‘fractus’ and the verb ‘frangere’. An object is said to be fractal if it is invariant under changes in scale; therefore, in one sense, a fractal set is said to be self-similar if a small part of it can be used to generate the whole of a larger version—like repeated photocopy enlargements of an image. A popular way of illustrating the meaning of ‘fractal’ is to ask how long a coastline is.

Table 1

List of some theoretical spherical distributions

**Von-Mise—Arnold—Fisher Polar distribution (Fisher, 1953)**

**Bipolar Dimroth—Watson distribution (Watson, 1965)**

**Equatorial distribution (Selby, 1964)**

**Bingham’s quasi-bipolar distribution (Bingham, 1974)**

**Small circle distribution (Bingham and Mardia, 1978)**

**Kent distribution (Kent, 1982)**

**Wood distribution (Wood, 1982)**

In a posthumous paper, Lewis Fry Richardson demonstrated that the answer depends upon the scale at which one starts. At progressively finer scales, it soon becomes obvious— as we encounter ever smaller details from bays down to coves, nooks and crannies, boulders, pebbles, sand grains, molecules, etc.—that a coastline has an infinite length within a finite area (Richardson, 1961). Incidentally, in 1922, Richardson gave us the famous verse

***“Big whorls make little whorls, which feed on their velocity;  
And little whorls have lesser whorls, and so on to viscosity.”***

in this oft-quoted parody of a verse about fleas upon fleas written by Jonathan Swift in 1733, Richardson was conveying another idea central to the notion of fractal geometry, i.e. self-similarity. Essentially, self-similarity is symmetry across scales or, conversely, pattern inside pattern, such that a small part of an object can be used to generate the whole of a larger version.

Fractals are not defined by a formal legalistic statement, but by the mathematical and graphical representations. A fractal can be quantified by its fractal dimension. Among the most fundamental fractal dimensions, which measure how efficiently a fractal, such as a coastline, occupies space, is the Hausdorff dimension,  $D_H$ , which is due to Felix Hausdorff’s pioneering work at the turn of the century on the area of geometry called topology (Hausdorff, 1919). A slight variant of  $D_H$ , and one of the most widely used in natural sciences, is the box dimension (or box-counting dimension or capacity dimension),  $D_b$ , defined by

$$D_b = \lim_{x \rightarrow 0} \frac{\text{Log}[N(x)]}{\text{Log}(1/x)}$$

where  $N(\mathbf{x})$  -called a hyperspace - is the minimum number of cells with side length  $\mathbf{x}$  on a grid needed to cover the fractal (coastline) at scale  $1/\mathbf{x}$ . To determine the fractal dimension of a two-dimensional field such as a forest perimeter,  $F$ , say, we superimpose a series of grids over a discrete range of scales and count the number of grid cells just touching or occupied by any portion of the forest perimeter, such that

$$D_b = \lim_{n \rightarrow \infty} \frac{\text{Log } N_n(F)}{\text{Log } (2^n)}$$

$N_n(F)$  is the minimum number of cells needed to cover the forest perimeter with grid cells of side length  $1/2^n$  ( $n = 1, 2, 3, 4, \dots$ ). For example, series of grids are scaled to  $N_1 = 4$ ,  $N_2 = 16$ ,  $N_3 = 64$ , etc. Each grid is laid over the forest patch and cells occupied by its perimeter are counted and plotted relative to the grid scale on log-log paper. The slope of the line of the series of counts is the fractal dimension of the forest perimeter. If  $D_b$  is not an integer, then  $D_b$  is said to be the fractal dimension of the perimeter  $F$ . There are many topologically related fractal dimensions for discs, cubes, spheres and mass, and many more that are an integral part of the mathematics of dynamical systems and statistics of chaos.

The magnitude of a fractal dimension reflects the dynamical and geometrical complexity of a system. It is also indicative of the number of degrees of freedom necessary to model the system. Apparently, fractals are products of dynamical systems and, therefore, provide an inextricable link between the mechanistic processes of wind and the resultant forest structure. However, mathematically, the link between fractals and dynamical systems is still uncertain, which partially explains why there is still so much difficulty in quantifying interscale relationships in forest— atmosphere interactions.

Considering that the science of fractal geometry is barely a decade old (although its initial concepts originated at the turn of the century), it is used extensively in statistics (especially time series analysis), physics, landscape ecology, economics, population biology and social sciences. Hydrologists and meteorologists are making a considerable contribution to the theory and application of fractal concepts in quantifying the interscale relationships of stream networks, rainfall, turbulent convection, fractal nature of clouds, multifractals of topography, etc. Obviously, fractal geometry is relevant to many aspects of agricultural and forest meteorology.

### ***3.1. Production geometry***

The drag coefficient and projected crown area of trees are two indispensable variates for modelling wind flow, fog interception, and other meteorological factors. Owing to a myriad of scaling factors within and between tree species and in under-story vegetation, it is virtually impossible to measure precisely their drag coefficients and projected crown area for all but the simplest components across a forest vegetation spectrum.

In a dynamical model, the drag coefficients must account for wind acting on a hierarchy of tree structures—root mass (anchorage), bark (fissured and smooth), boles, boughs, twigs, buds, foliage (none for deciduous species in winter), veins, stomata, and cone or fruit mass. Consideration must also be given to changes in the structure owing to loading by many factors, such as predation, freezing rain, snow, plus innumerable thigmomorphogenetic responses to wind such as the development of cones, contortions of trunks, subnival shoots and wood properties (spiral grain, moisture content, wood density variability, and compression or tension wood). These and many other features of tree and stand architecture are rarely considered in biomechanical models.

Obviously, the many degrees of freedom required to model realistically the dynamics of wind acting on a (whole) tree is beyond the realm of most computers. Consequently, forest meteorologists (and mensurationists) generally, for convenience, concentrate on simplified models that reduce tree shapes to simple convex hulls (i.e. with smooth surfaces).

Oldham (1992) suggested a fractal-based ‘production geometry’ model for the design of agroforests. He made the analogy between the fractal geometry of the porous Menger sponge and an agroforest. The most distinctive feature of a Menger sponge is its lacunarity (a term also coined by Mandelbrot for quantifying spaces within an object) with a distinctive hierarchy of spaces (Fig. 4).

Such a concept would incorporate complex dynamics in a model of agroforests including simulations of scaled systems hierarchies, such as those encountered in projected crown area or, conversely, the spaces within the forests, besides the stochastic and chaotic dynamics inherent in the non-linear nature of wind effects on the forests in general.

Although there are many expressions of fractal dimension,  $D_b$ , they are all topologically and mathematically related. Fractal dimensions are either exact or statistical: those that have a regular geometry such as circles, squares, convex hulls (cylinders, spheres and cones) and the Swiss cheese-like Menger sponge are exact fractals, whereas the irregular shape of a tree (projected crown area, leaves and branches, fissured bark, etc.) and stand architecture, shorelines and river networks are statistical fractals. Milne (1991) gave a particularly good treatment of the application of fractal models to studies of landscape dynamics, and Turner et al. (1989), in a study on predicting the spread (percolation) of disturbance processes on landscape heterogeneity, showed how the degree of  $D_b$  is related to disturbance intensity and percolation thresholds in landscape heterogeneity. Essentially,  $D_b$  is a function of disturbance intensity. For example, an abrupt increase in  $D_b$  is indicative of a phase change caused by moderate to high disturbance intensities in common disturbance-susceptible landscapes as the shape of the largest cluster within the landscape unit becomes more complex (rougher). Obviously, fractal models of this type have considerable potential for understanding pattern and process in wind-shaped forests.

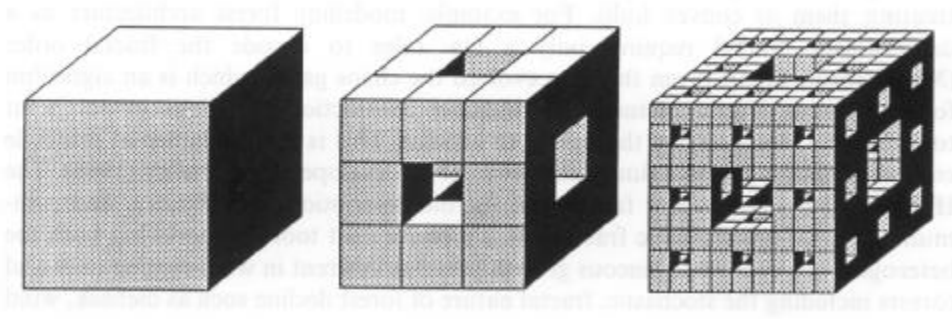


**Fig. 4. The Menger sponge—a ‘regular’ fractal illustrating the principle of self-similarity. To construct a Menger sponge, subdivide the faces of the initial cube into nine congruent squares to give 27 cubes and remove the centre cube. Then subdivide the eight smaller cubes into 27 smaller cubes and remove the middle cubes as before; and so on, *ad infinitum*.**

### 3.2. Thin fractals

As explained above, the box dimension,  $D_b$ , is useful for calculating the fractal dimension of perimeters. The perimeters are usually treated as thin fractals (infinitely thin lines) with a fractal dimension between one and two, and are useful for measuring the tortuosity of a curve in a plane, such as a river, forest edge, crown or stand profile, tree ring time series and the scaling properties of bifurcations in river networks.

However, Zeide and Pfeifer (1991) contended that  $D_b$  is inefficient for measuring the fractal dimension of tree crown profiles. Alternatively, they devised a two-surface method by which the fractal dimension is expressed as the relationship between the leaf area of a tree and the surface area of the convex hull that envelops the crown.

### ***3.3. Fat fractals***

Ian Stewart's comment that "We are not walking blood-bags—we are fractais incarnate!" (Stewart, 1992) rings true in the volumetric fat fractal model of the blood circulation in the human body developed by Grebogi et al. (1985). The fat fractal model has been adapted to many other fields, particularly hydrology. For example, the fat fractal of a drainage basin is the total area of the basin minus the surface area of river channels. This approach should be appropriate for forest meteorological phenomena with well-defined planar pathways, such as corridors through forests and surface wind flow patterns (channelization). Potentially, this concept can be applied to hydraulics of trees to provide models of the relationships of biometeorological processes such as evapotranspiration and translocation of biochemicals as a function of wind.

### ***3.4. Wind-shaped fractal forests***

It is unlikely that trees and forests are entirely fractal (self-similar) any more than there is such a creature as an 'average' forest. Nevertheless, as we do in averaging, treating certain aspects of trees and forests as fractal is more advantageous than treating them as convex hulls. For example, modelling forest architecture as a deterministic fractal requires only a few rules to decode the fractal order (Mandelbrot, 1983). From this idea evolved the chaos game, which is an algorithm for computing fractal pictures and includes contraction mappings or set point topology, i.e. compressing the fractal to a point. This is the fundamental principle embodied in the iterative function system (IFS) developed by Barnsley (1988). The IFS provides a convenient framework for the description, classification and communication of deterministic fractals. It is a convenient tool for modelling both the heterogeneous and homogeneous growth patterns inherent in wind-shaped trees and forests including the stochastic, fractal nature of forest decline such as dieback, wind throw and wind snap.

There is a close relationship between the fractal dimension of trees and site quality. On a poor site with extreme environmental stress, trees have heterogeneous (asymmetrical) profiles with high fractal dimension, whereas on good sheltered sites trees tend to have homogeneous (symmetrical) profiles with a low fractal dimension (Zeide, 1993). Fractal-based mensurational models also provide good estimates of tree mass without the necessity of destructive sampling. For example, Zeide and Pfeifer (1991) calculated the fractal dimension of ten Rocky Mountain coniferous tree species by regressing the crown form factor on crown volume, crown length and width. Similarly, the fractal dimension of a crown can be derived by regressing foliage area (mass) on the area of the convex hull that envelops the crown (Zeide and Gresham, 1991). Collectively, these studies show that the fractal dimension of individual trees is controlled by competition, such that the crowns of dominant trees have a higher fractal dimension than intermediate and suppressed trees because they have a higher proportion of foliage mass.

Because Zeide's model considers only the symmetrical case for convex hulls, it would provide no information on the asymmetric growth response to strongly directional mechanistic processes such as the influences of meteorological factors (wind, snow, glaze, fog, radiation, etc.).

This problem is partially resolved in the fractal-based graphical models developed by Chen et al. (1993). Heterogeneous and homogeneous growths are implicit in their simulations of poplar trees with different branch structures and variations of five basic leaf angles, leafiness with respect to day of the year, and leaf area index. Other aspects of short-rotation poplar stands are simulated, including crown and stand architecture, gap fraction and leaf normal inclination distribution in relation to light regimes and other ecophysiological factors. At much finer scales, Korn (1993) evaluated the fractal dimension of the outline of a colony of algae and developed a fractal computer model to simulate the heterogeneous growth of plant tissue.

### 3.5. Multifractal forests

Within the last few years there has been a spate of models of scale invariance and multifractal cascades in atmospheric phenomena, such as turbulence, rainfall, radar reflectivities, cloud fields and topography. A simple example of a multifractal field is the variation of fractal dimensions between individual isolines such as elevation contours. For example, fractal dimensions of unstable scarps at the crest of mountains would exhibit rougher contours than the stable lower slopes. Similarly, edges within a forest damaged by wind tend to have a higher fractal dimension than undamaged edges; hence, the forest as a whole is a multifractal.

Functional box counting analysis, defined by Schertzer and Lovejoy (1991), can characterize scaling functions. As its name implies, it is a box counting method which stratifies the cascade by transforming the multifractal field,  $f(x)$ , to exceedance sets such that the number of boxes to cover,  $A_T$ , is defined by the threshold,  $T$ , such that

$$T: \{A_T \mid f(x) > T\}$$

and

$$A_T: N_T(L) \approx L^{-D(T)}$$

where  $N_T$  is the number of boxes whose value exceeds  $T$ , at length scale  $L$ , and  $D(T)$  is an estimate of box fractal dimension.

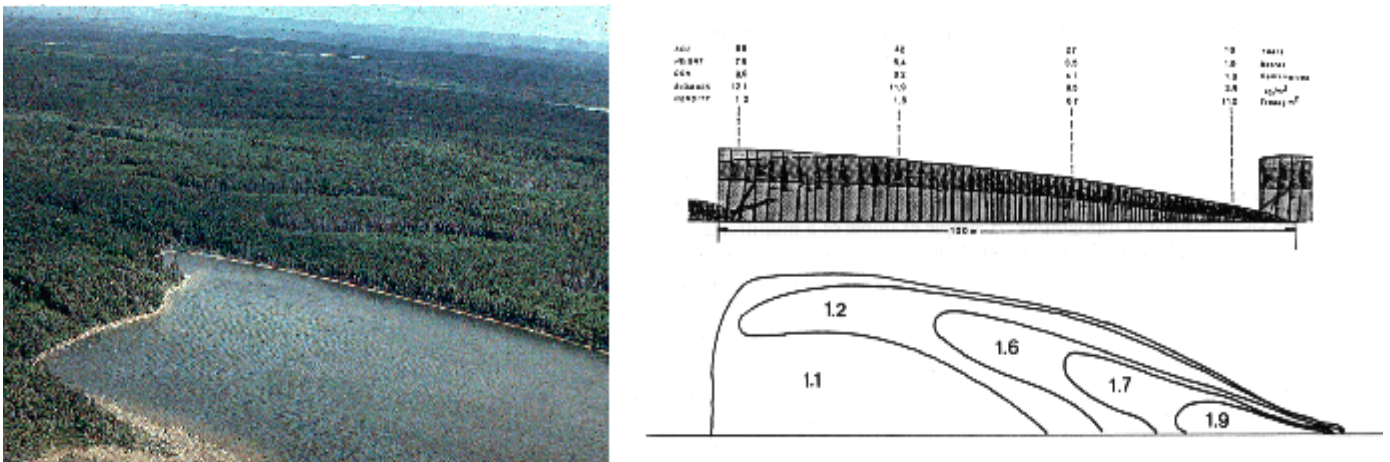


**Fig. 5.** Top: a section of a wave forest at Spirit Cove, Newfoundland, showing a pair of well-defined wave cycles with their characteristic dead tree strips followed by mass regeneration. Because of the patterns of vortex shedding, the motion of wave cycles is almost perpendicular to and away from the shoreline. The streaks of foam perpendicular to the wave motion on the pond are Langmuir streaks, i.e. helical roll vortices (see text on how similar vortices may shape the wave forest). Centre: a schematic representation of the profile of a well-defined wave cycle. Bottom: the box counting (fractal) dimension illustrates the multifractal nature of a wave forest cycle (the fractal dimensions were derived from ~fractal pictures' of a wave cycle using the IFS algorithm).

## 4. CHAOS: PATTERNED INSTABILITIES

In parametric statistics, it is considered that variances are normally distributed and that most events are potentially predictable. However, tests for normality may be inappropriate or unnecessary, as the parameterization of many non-linear interactions between wind and forests cannot easily be estimated if the sampling distributions cannot be derived by statistical analysis.

Statisticians have developed many ways of resolving such problems such as distribution-free and robust statistical methods (Potvin and Roff, 1993), or choose from a family of parametric statistics which focus specifically on the heterogeneity of errors (e.g. Vautard and Ghil, 1989; Burroughs, 1992). Alternatively, we could apply the new techniques of statistical chaos theory with its capability of describing very complex processes with simple parsimonious models and essentially without error (Chattargee and Yilmaz, 1992).

Colloquially, chaos means formless matter, disarray, confusion. In dynamical systems theory it usually means non-random (ordered) but unpredictable, or, synonymously in aerodynamic terminology, a patterned instability.

Many consider chaos theory to be the most important discovery since relativity and quantum mechanics. In physics, meteorology, climatology, engineering and chemistry such euphoria may be justifiable. Others are not quite so exuberant, and at least one scholar commented that “to accept chaos is to accept defeat”. Smith (1991), more realistically, stated that “in areas such as ecology and economics, it is impossible to know the detailed mathematical equations governing the system; and the whole of the evidence for ‘chaos’, if indeed there is any evidence at all, comes from the interpretation of experimental data”.

The well-known fact that the most powerful computer in the world cannot solve the Navier—Stokes equations for any but the simplest (laminar) flows confirms Smith’s first point. His second point is philosophical. For there is no more precise a description of chaos than there is a complete mathematical solution to turbulence or a single definition of fractal. But who would deny the existence of turbulence or the attributes of fractal geometry? The nature of chaos as a physical, mathematical, statistical, biological and meteorological phenomenon has been described and modelled extensively in Mullin (1993). Other particularly good treatments on the methods and application of chaos theory are those provided by Hastings and Sugihara (1993) on the natural sciences and by Peters (1994) on investment and economics. Indeed, there are many examples of simple deterministic models that show how irregularity can be generated with only a few degrees of freedom interacting non-linearly to create ‘chaos’. Also, literature is replete with statistical models that describe or come tantalizingly close to describing randomness that results from a known partially deterministic (chaotic) process. However, according to Chattargee and Yilmaz (1992), that is still only a possibility.

This means that if a dynamical system is inherently chaotic then its description may not require complex models. For example, a study of interscale relationships in ecodynamics by Holling (1992) shows how a few dominant frequencies (degrees of freedom) can entrain other lesser processes. Intuitively, the constant-canopy biospheric models widely used in remote sensing operate in much the same way by focusing on ‘effective parameters’ while ignoring the effects of small-scale landscape heterogeneity on the large-scale energy fluxes in atmosphere—land interaction (Wood and Lakshmi, 1993). Similarly, a few dominant parameters, namely, human impacts and, to a lesser extent, five hydrogeomorphic variables, characterize the fractal shape of riparian forest patches along the Cedar Rivers, Iowa (Rex and Malanson, 1990).

Concentrating on dominant degrees of freedom gives the advantage of describing at least the macro-mechanisms such as the principal pattern-forming instabilities associated with wind-shaping of forests, although the micro-mechanisms may never be entirely predictable. For example, it is not difficult

to categorize forest types that are susceptible to wind throw, or the probability of storm frequency in a particular region. If, however, these events are inherently chaotic then, as with the Navier—Stokes equations, only short-term prediction of their simplest frequencies is possible.

#### *4.1. Dimensions of chaos*

In practice, it is difficult to distinguish between stochasticity (pure randomness) and chaos. First, in biophysical systems, stable and unstable dynamics are interwoven in complex patterns, so it is not known at the outset where the chaotic regions lie. Second, chaos occurs in segments, therefore only short-term prediction of it is possible. Third, as there are no statistical tests for chaos in the traditional sense of hypothesis testing (Berliner, 1992), chaos cannot be identified by the methods of classical time series analysis.

Chaotic dynamics are better understood by representing time series using an embedding procedure to create a mathematical space called a phase space so as to see its attractor. There are two kinds of attractors—the so-called classical attractors (fixed point, circle, torus), which are manifolds, and strange attractors, which are fractal. Mullin (1993) and Stewart (1992) gave a good brief and lucid description of attractors. To use their analogy, imagine rolling a golf ball inside a car tyre. Let the ball roll down one side of the tyre wall and it will come to rest at the bottom of the tyre. If we project the trajectory of the ball onto a piece of paper below it would settle to a fixed point which we call the fixed point attractor (we call the plot of the trajectory a phase portrait). Next, let the ball roll around precisely on the bottom of the tyre; its phase portrait would show a circle attractor. Then roll the ball so that it winds around the inner walls of the tyre; the phase portrait would then display a torus attractor. If we magnified segments of a torus they would appear flat and unlike each other. By contrast, the segments of a strange attractor retain the essential features of nested tori, i.e. it is self-similar and therefore fractal. So when we search for chaos, we examine whether the attractor is classical or fractal. The first strange attractor identified as such is the famous Lorenz ‘owl mask’ attractor (actually derived by Ed Lorenz’s collaborator Barry Saltzman while working at Yale University) (Lorenz, 1963). Although there is still no formal proof that it is a strange attractor, it is the first example of chaos in meteorology or ‘deterministic non-periodic flow’ as Lorenz called it. Many years had passed before dynamical systems theorists and mathematicians became aware of the significance of the Lorenz attractor as one of the cornerstones of chaos theory.

Among our primary goals is to distinguish between stochastic processes and deterministic chaos in a time series. One way to approach this is to analyse the structure of the phase space. So, to get at the attractors, a phase space is created by an embedding process which contains the essential information of the original state-space in the time series. If chaos exists, then plotting trajectories in a phase portrait reveals the structure and dynamics of its underlying strange attractor (Field and Golubitsky, 1992).

To detect and characterize strange attractors, the usual approach is to use a hierarchy of topologically related fractal dimensions to examine whether, for example, the relationship between the correlation dimension,  $D_c$ , and the embedding dimension,  $D_e$ , is linear or non-linear. If the relationship is linear, then it is usually a stochastic (random) process. A non-linear curve that increases and becomes constant at a certain level suggests deterministic chaos. Several algorithms for computing the fractal dimensions of data structures are required to derive  $D_c$  and  $D_e$ . Because chaos theory is mathematically complex, it is only possible to provide a sketch of the more widely used, albeit imperfect, dimensions of strange attractors that may provide clues to whether a time series is chaotic or not. For the broad view of their practicality and pitfalls with respect to research on meteorology, climatology, turbulence, and biology, Mullin (1993) is highly recommended. The following are some of the principle dimensions used to characterize strange attractors.

### 4.2. Capacity dimension, $D_b$ ,

The capacity dimension,  $D_b$ , described above, is one of the simplest approaches for characterizing strange attractors. However, instead of boxes, it is formulated for hypercubes, i.e.

$$D_b = \lim_{\epsilon \rightarrow 0} \frac{\log N(\epsilon)}{\log(1/\epsilon)}$$

The capacity dimension is calculated by successively dividing the phase space with  $D_e$  into equal hypercubes,  $N(\epsilon)$ , of linear size  $\epsilon$  required to cover the attractor and plotting the logarithm of the fraction of hypercube that is occupied with data points vs. the logarithm of the normalized linear dimension of the hypercube. The average slope of the line for the two middle segments is taken as the capacity dimension. Although the concept is simple enough, computation requires a large computer memory.

### 4.3. Correlation dimension, $D_c$

This dimension is due to Grassberger and Procaccia (1983), and is more efficient than the capacity dimension. It is formulated in much the same way as  $D_b$ , but instead of hypercubes, we use hyperspheres ( $N(r)$ ) with radius  $r$ :

$$D_c = \lim_{r \rightarrow 0} \frac{\log C(r)}{\log r}$$

where the hypersphere  $C(r)$  is an average point-wise mass, or correlation integral, defined by

$$C(r) = \frac{1}{N^2} \sum_i^N \sum_j^N H(r - |X(t_i) - X(t_j)|)$$

where  $H$  is the Heaviside step function (number of points within radius  $r$ ),  $N$  (the total number of points) is the number of points ( $x_i, x_j$ ) within the hypersphere such that

$$|X(t_i) - X(t_j)| < r$$

If the relationship  $C(r) \approx r^{D_c}$  exists for sufficiently small  $r$ , then  $D_c$  becomes the correlation dimension of the attractor. In other words,  $D_c$  is the fractal dimension of the strange attractor. Of course, the correlation dimension does not in itself always 'prove' the existence of chaos, but it does provide an initial starting point for doing so.

### 4.4. Embedding dimension, $D_e$

$D_e$  is a time-lagged process to determine the fractal dimension of the time series vector. A pleasing analogy by Sugihara et al. (1990) likens embedding to dragging a garden fork sideways across the time series. The constant  $r$  is a delay time analogous to the number of prongs of the mathematical garden fork. If time series have an equal time interval  $X_{it}$ , the vector time series is defined

$$\mathbf{X}_{ij} = \{X_{ij+T}, \dots, X_{ij+T}, \dots, X_{ij+T+D_e-1}\}$$

where  $r$  and  $D_e$  are the delay time and the dimension of the vector, respectively.  $T$  can be chosen in a range from values larger than the sampling time interval but smaller than the autocorrelation time of the time series. The dimension of the vector is  $2D_T + 1$ , where  $D_T$  is the topological dimension of the strange attractor (Takens, 1981).

#### 4.5. Lyapunov exponent, $A$

$A$  is a measurement of the sensitivity to initial conditions and quantifies the average exponential rate of divergence or convergence of points with nearly identical initial conditions. Thus, it provides an indication of how far into the future reliable predictions can be made. If  $A > 0$  and large it is usually an indication of rapid divergence (chaos). Conversely, if  $A \sim 0$  and large (more negative) it indicates rapid convergence towards a stable state (Wolf et al., 1985). Values of  $A$  close to zero indicate periodic states.

#### 4.6. Information dimension, $D_i$

The information dimension,  $D_i$ , also called Shannon's entropy, is the scaling exponent in the variation of entropy, i.e. the Kolmogorov entropy, which measures the loss of information as a chaotic system develops. In other words, it characterizes the transition between stochasticity and chaos. Hence,  $D_i$  describes phase changes such as transient dynamics. To calculate  $D_i$  one essentially counts the repetitions of a pattern in a time series during phase changes. Wang and Gaspard (1992) provided a generalization of  $D_i$  as it applies to the cascade process of turbulent eddies. They showed that  $D_i$  can distinguish between various stochastic processes in the phase transitions from periodic oscillation, temporal chaos, soft turbulence, hard turbulence and fully developed turbulence. More importantly, they showed that different states of turbulence have a higher degree of stochasticity than chaotic states because of scaling factors of  $D_i$ .

Fig. 6 shows the correlation integral,  $C(r)$ , for a range of embedding dimensions,  $D_e$ , from three to eight (left to right) obtained from a periodic time series and time series of wind speed and wind direction at Daniel's Harbour, western Newfoundland. Fig. 6 basically illustrates the difference between invariance, a strange attractor (chaos) and pink noise.

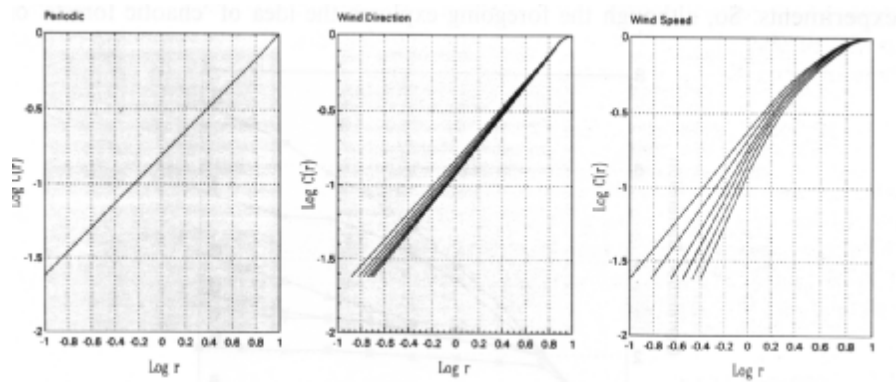


**Fig. 6. Log—log plots of the correlation integral,  $C(r)$ , vs. hypersphere of radius  $r$  for a range of embedding dimensions (three to eight—left to right within the centre and left graph) using time series of average hourly wind direction and wind speed at Daniel's Harbour, western Newfoundland, and, for comparison, a periodic time series. In the periodic case the slopes of embedding dimensions 3—8 are coincidental, as one would expect for a classical (invariant) attractor. As one would expect, veering of wind direction associated with the passage of weather systems results in a patterned but unpredictable time series similar to chaos, as indicated by close, slightly divergent curves. The wind speed time series is characteristically pink noise resulting from the turbulent cascade as energy is transferred from larger-scale to smaller-scale structures. Graphically, the pink noise is reflected in strongly divergent curves.**

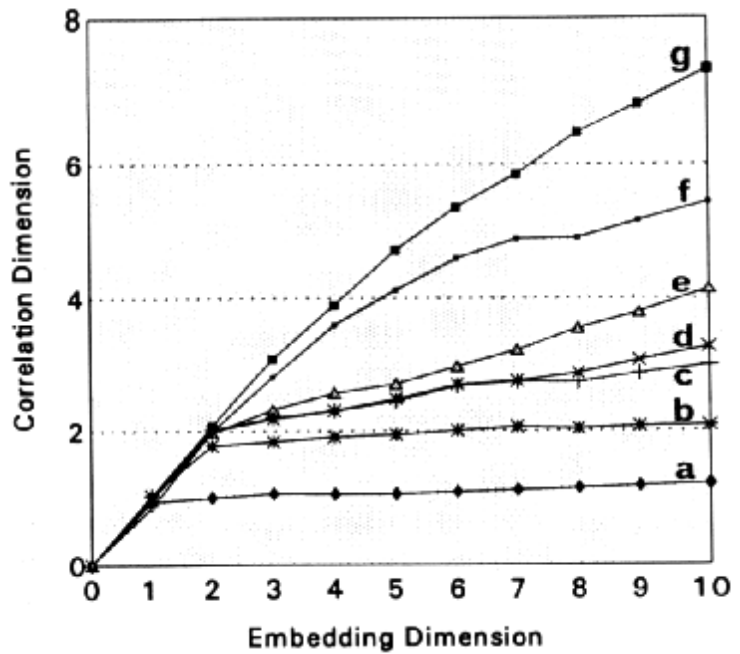
The six curves for a periodic time series are coincidental, i.e. invariance of classical attractor. On the other hand, the curves for wind direction diverge slightly at lower embedding dimensions, but at higher embedding dimensions are virtually parallel. In this case, the time series has a strange attractor and therefore would be chaotic, or close to being chaotic.

This is a reasonable assumption, because the structure of wind direction time series from a coastal site tends to contain well-defined patterns that are predictable in the short-term embedded within unpredictable (random) segments resulting from the passage of weather systems. By contrast, the curves for wind speed diverge and decline rapidly. This suggests that the structure of the time series is pink noise, as one would expect in a wind speed profile that reflects the turbulent cascade as energy is transferred from large-scale to smaller-scale structures.

Fig. 7 plots the correlation dimension,  $D_c$ , vs. the embedding dimension,  $D_e$ . Of several time series representing different types of data. As stated above, if the slope is linear it indicates a stochastic (random) process, whereas if it is non-linear and saturates (i.e. when  $D_e > D_c$ ) then  $D_c$  will (more or less) remain at a constant level. Fig. 7 is intended to provide a perspective on hierarchy of predictability that one would expect from a range of 'typical' vs. 'statistical' time series. From the lowest to the highest curve we have: (a) a periodic series generated by a sine function; (b) the patterned but unpredictable chaotic structure of the Lorenz attractor; (c) the structure of wind speed (measured at 3 mm intervals and integrated over 15 mm) at Gunnarsholt, south Iceland, after taking fourth differences of the raw data, which suggests elements of chaos; (d) Swedish tree-ring time series having a similar structure to (c); (e) average hourly temperature measured at Pasadena, western Newfoundland, during late winter to early spring (February-April); (f) 'noisy' structure of raw wind data from Gunnarsholt; (g) a typical stochastic time series generated by a random process.

Characterizing strange attractors or, more to the point, recognizing chaos is rather difficult to achieve beyond the simplicity of time series analysis or laboratory experiments. So, although the foregoing explores the idea of 'chaotic forests' one should keep in mind that, although patterned instabilities are commonplace in nature (perhaps the rule rather than the exception), there is much work to be done before we can quantify them as such. Part of the process will undoubtedly involve a major refurbishing of existing fractal dimensions and perhaps even a new set.

**Fig. 7. Correlation dimension,  $D_c$ , as a function of embedding dimension,  $D_e$ , for time series with different structures; (a) periodic; (b) chaos; (c) 15 mm average wind speed (after taking fourth difference) at Gunnarsholt, Iceland; (d) Swedish tree rings widths; (e) 30 mm average temperature profile at Pasadena, Newfoundland (February-April); (f) same data as in (c) before differencing; (g) stochastic (random).**



## 5. CHAOTIC WAVE FORESTS

If there is a forest analogue of a dynamical system that best fits the description of a patterned instability it is the peculiar wind-shaped wave forest phenomenon. However, proving the case for a chaotic wave forest may not be an easy task. First, as Green (1991) noted: “dynamical systems are inherently evolutionary and historical and, therefore, irreversible insofar as the sequence of events cannot be retraced precisely”. Second, the patterns and properties of wind in relation to other environmental factors primarily responsible for creating and maintaining wave forests are difficult to quantify.

Wave forests, also called wave regeneration and wave dieback, have been known in Japan for centuries, particularly in subalpine fir forests on Mt. Shimagare, which translates literally as the ‘mountain with the dead tree strips’ and in northeastern North America. Until the mid-1980s they were considered to be extremely rare outside the three principal areas where they occur (Newfoundland, Adirondack Mountains of USA, and northern Japan). However, many reports of forest instability indicate that some features of a typical wave forest dynamics, such as progressive dieback in forest edges, are common in coniferous forests and plantations throughout the world, and result from the combined effects of wind and humans. In many regions of the world, prime timber is lost to forest edge erosion specifically and forest instability generally (Robertson, 1993b). Therefore quantifying the primary meteorological factors involved in wave forest phenomena is of considerable economic and environmental importance. In this respect, there are several fundamental questions:

- (1) **Is the frequency and distribution of wave forests in a region a function of long-term changes in the pattern of weather systems (namely storm tracks) or short-term changes in local wind regimes?**
- (2) **Where does a wave forest fit in the evolution of forest ecosystem dynamics?**
- (3) **What are the principal biometeorological factors that create and perpetuate wave forest?**
- (4) **Are wave forests stochastic, chaotic, or quasi-periodic dynamical systems?**

The short answer to these questions is, we do not know! There are no measurements, or dynamical systems models or simulations of the aerodynamics and other meteorological factors that would create and perpetuate a wave forest. Nevertheless, there are a number of studies of the ecodynamics of wave forests that give a general indication of the relative impact of some of the meteorological factors. The following discussion, which may shed some light on these questions, is restricted to four contrasting types of wave forests in Newfoundland; namely, a wave krummholz, and coastal plain, mid-slope and valley wave forests.

### ***5.1. Converging storm tracks***

There is an eastward travelling ‘wave-like’ pattern in the mid-latitude weather systems, which exhibits a degree of coherence within a more disturbed open system that occurs within distinctive geographical regions noted for the passage of storm tracks (Read, 1993). The Province of Newfoundland and Labrador lie within one of those regions dominated by weather disturbances.

Stated another way, weather systems in the interior of North America are more predictable than the generally unstable weather systems associated with the passage of frontal systems in the northeastern maritime region. As the principal tracks of frontal systems over North America and the western Atlantic Ocean tend to converge toward eastern Canada, the surface wind flow would allow less well-defined patterned instabilities but essentially retain the characteristics of smaller-scale chaotic flow. If this is so,

then perhaps the 'chaotic' wind flow should in some way be reflected in the temporal and spatial heterogeneity of eastern forests including wave forest phenomena.

## 5.2. *Chaos in tree rings*

At a finer scale it is reasonable to expect that analysis of tree ring time series would establish the relative impact of weather systems on forests. Certainly, it is well known that tree ring time series of trees growing in the relatively stable climate of the continental interior of North America are generally not as 'noisy' as their counterparts growing in insular climates along the northeastern seaboard. Also, the Boreal coniferous forests in humid, windy eastern maritime regions tend to have a lower stature but have a much more dynamic, younger, heterogeneous structure and are richer in biodiversity than Boreal forest in drier, less windy continental regions. The extreme dynamism of maritime Boreal forests is reflected in the extreme variability of tree ring patterns.

Burroughs (1992) gave many examples of spurious relationships between natural events and weather cycles derived from time series analysis, including dendroclimatology. Also, Blasing et al. (1984) stated: "Decisions about the number of climate variables to include, the confidence limits, number of eigenvectors to allow as candidate predictors in regression, etc., can affect the response function in unpredictable ways and lead to possible errors in interpretation."

Van Deusen (1989) showed how traditional models of simple averaged time series in tree ring chronologies can be misleading. Consequently, he introduced two recursive models similar to the logistic models used by May (1976) that are synonymous with chaos theory. He also emphasized that dendrochronologists must come to terms with chaos if they are to gain a better understanding of environmental influences on tree growth.

In coastal and subalpine coniferous forests of northeastern North America major winter weather events, such as frequent storms and episodes of freezing rain and warm weather causing snow melt, affect tree growth for many years afterwards. On the positive side, regeneration and juvenile growth on sheltered sites is exceptional. However, the negative effects of weather on trees and forests become obvious as trees mature.

The crowns of conifers are especially prone to winter damage; notably, desiccation (winter burn), branch and needle abrasion by winds laden with ice crystals, and damage by wet snow or freezing rain that annually strips a substantial proportion of buds, foliage and twigs from conifers, and twigs and branches from deciduous trees. In addition, and impossible to observe directly, is recurring fine-root mortality caused by freeze—thaw cycles and wind shake. Added to these effects are the ecodynamics of competition, ageing and predation (Robertson, 1993c). Naturally, prior tree-growth variables also mask climatic effects. Although Blasing et al. (1984) showed how a correlation function can be useful in detecting the masking, it is, nevertheless, with the exception of wind, virtually impossible to extract climate and weather signals from 'proxy' data from trees in coastal boreal climates.

The distinctive directionality of wind frequencies leaves an indelible signature in the asymmetric patterns of tree ring width and wood properties such as the circular variability of density and location of compression wood within the boles of wave forest trees (Robertson, 1991). However, even if chaotic wind begets chaotic tree rings, it is unlikely that such a relationship will be found in the tree ring patterns of a wave forest tree. First, to establish that chaos exists, a time series with at least 1000 points is required to generate any semblance of a strange attractor in a phase portrait. Second, dominant trees in wave forest begin to decline at 30 years of age and die at around 50-60 years.

Alternatively, longer-lived species in proximity to the wave forest could serve as surrogates. However, although deciduous trees (birch) attain ages of 200-300 years, they too are in poor form before they are 100 years old. Nevertheless, 200 points are enough to obtain at least an indication of chaos in a time series structure. An exploratory study of a pair of tree ring time series (Fig. 8), selected from birch

trees sampled in coastal areas of Newfoundland, indicates that at least one may have chaotic segments (A. Robertson, L. Lye and B. Wu, unpublished data, 1993). Using standard time series analysis, the structure of one of the tree ring time series was classified as a stochastic process, the other as fractional Brownian noise. Fig. 8(a) shows that the Hawke's Bay time series is a 'noisy periodic' bistable stochastic process with a relatively high frequency, and that its two distinctive periods have essentially the same structure. The bifurcation point at year 1889 is a phase change that could have resulted from one or more biophysical factors (loss of branches from freezing rain or storm damage) or a diminished growth response to an abrupt ecosystem change (abrupt mass regeneration of balsam fir, or predation).

By contrast, the Bay d'Espoir time series consists of mainly fractional Brownian noise and, with a large positive Lyapunov exponent and a correlation dimension less than five, is indicative of a strange attractor, i.e. low-dimensional chaos (Fig. 8(b)).

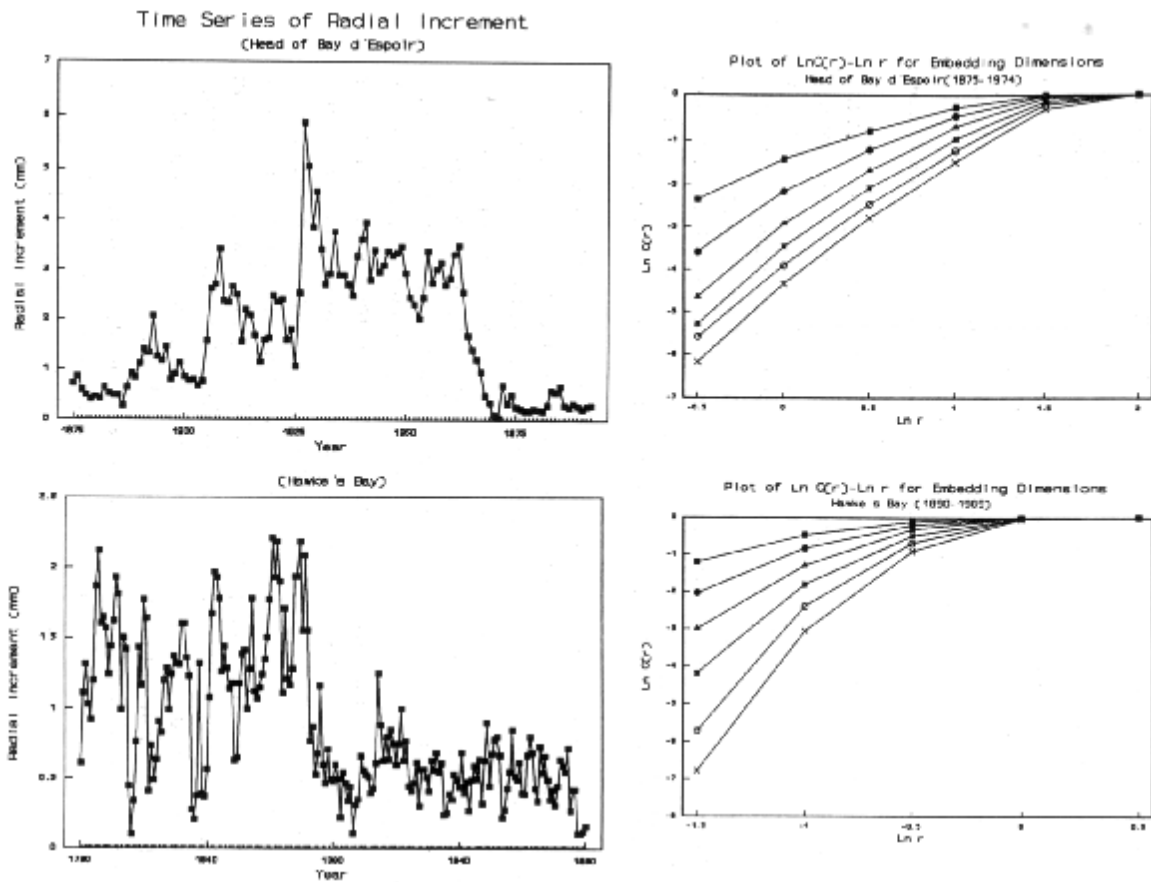


**Fig. 8.** Tree ring time series from a yellow birch growing on a sheltered site at the Head of Bay d-Espoir in southern Newfoundland (top left) and a mountain paper birch growing on a relatively windy site near Hawke's Bay on the coastal plain of the Great Northern Peninsula (bottom left). Corresponding plots of the correlation integral of the Bay d'Espoir time series may have a strange attractor (chaos), as indicated by the virtually parallel curves at higher embedding dimensions (top right), and the Hawke's Bay time series is a 'noisy' bistable process, as the curves diverge rapidly. However, both time series are too short to determine if either has a strange attractor or not using current chaos models. (Source: A. Robertson, L. Lye and B. Wu, unpublished data, 1993).

### 5.3. Chaotic wave forests

Dynamically and geometrically, a wave forest is, in essence, the biological analogue of turbulent eddies that form a roll vortex, which are suspected of having a role in the creation of wave forests. In its most simple and well-defined form a wave forest is defined as: a monospecific forest with a series of canopy edges, characterized by mass dieback and mass regeneration, moving across the landscape in wave-like formations in a more or less predictable cycle.

However, many variations of wave forests only partially fall within the definition, particularly those initiated by human activities, such as forest edge dieback as a result of clear cutting, construction of roads, power corridors, settlements, etc. Here we will concentrate on natural wave forests.

There are hundreds, if not thousands, of examples of wave forests in Newfoundland and southern Labrador. Fig. 9 shows the location of a few well-defined wave forests in Newfoundland. Four contrasting examples of coastal wave forests in Newfoundland are the wave krummholz at L'Anse-au-Claire (1), the coastal plain wave forest at Spirity Cove (2), the wave forest on the upper slopes at Birchy Lake (5) and the valley wave forest at Ship Cove (7). Each wave forest complex appears to have been created by different patterns of vortex shedding.

The wave krummholz, on a southwestern slope of a long narrow ridge at L'Anseau-Claire is approximately 2 m high. As the trees do not produce seed, the krummholz regenerates vegetatively from subnival shoots. The most likely explanation for the bands of dead tree strips is that they result from vortex shedding by strong northeasterly winds that intercepted along a sharp ridge at approximately 30\_400 angle. The vortex shedding results in bands of longitudinal lee vortices. Naturally, these vortices would cause snow deposition and freezing rain to occur in bands that may accentuate and perpetuate the wave krummholz.

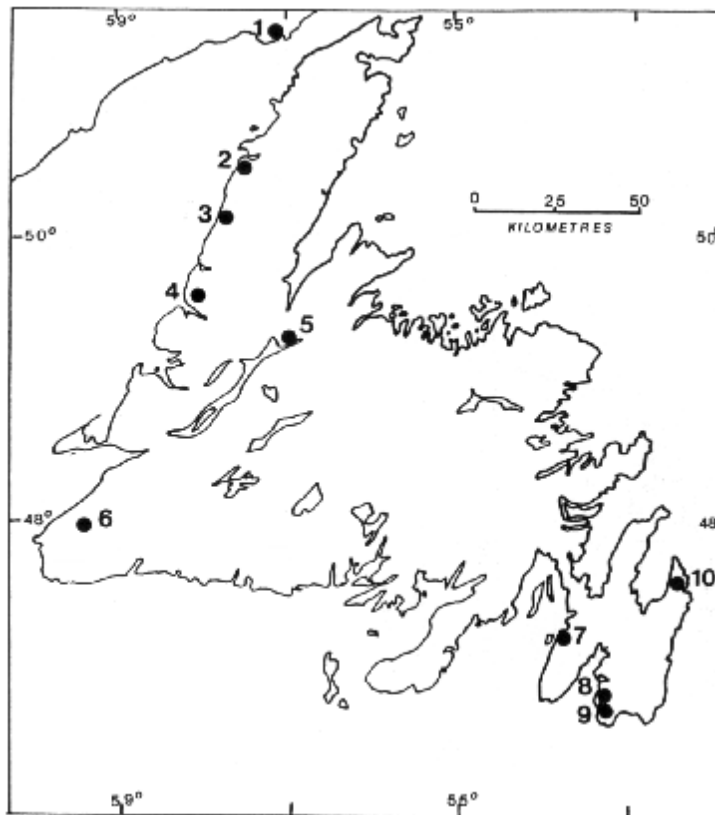


**Fig. 9. Map of Newfoundland showing a few locations of classic examples of wave forest phenomena. 1, Lance-au-Clair; 2, Spirity Cove; 3, Daniel's Harbour; 4, Rocky Harbour; 5, Birchy Lake; 6, Anguille Mountains; 7, Ship Cove; 8, Gaskiers; 9, Peter's River; 10, Torbay.**

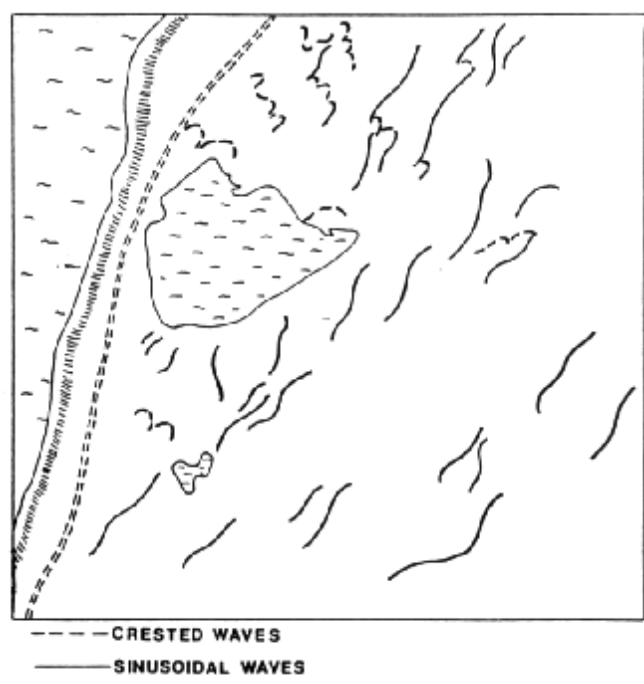


**Fig. 10. Two contrasting types of wave forests in Newfoundland showing the birth of a wave forest revealed by the light patches of dead tree strips on the upper slopes above Birchy Lake (top), and part of the well-established Spirit Cove wave forest (the patterns of crested and sinusoidal dead tree strips are plotted for simplicity (bottom right). In both cases, the motion of wave forests is from left to right (with the exception of crested dead tree strips in (b), which move towards the top at an angle of roughly 45°).**

The wave forest on the coastal plain at Spirit Cove (Fig. 10(a)) is unique because the low, gently sloping landscape is incapable of generating strong lee vortices. However, the fact that the alignment of the principal axes of longitudinal vortices and of the sinusoidal dead tree strips is virtually parallel may be significant. On days with strong winds from the west-southwest, the presence of convective longitudinal helical roll vortices generated offshore on the Gulf of St. Lawrence is indicated by streaks of foam (Langmuir vortices) 2—20 m apart on the surface of lakes and rolling bands of turbulence or ‘ripples’ on the ocean 100—500 m apart. Longitudinal helical roll vortices are geometrically similar to Taylor vortices, particularly the band-like wavy Taylor vortices. At the ocean—land interface they would become

irregular, like turbulent Taylor vortices, and further inland, these would undergo further transformation into less well-defined vortices, perhaps akin to Honami waves, owing to the influence of roughness elements and convective fluxes.

The Ship Cove wave forest is characterized by crescent-shaped dead tree bands as opposed to the sinusoidal strips at Spirit Cove. This indicates that it is a young (100-150 years old) and extremely dynamic system that is maintained primarily by westerly gale-force wind, rather than prevailing southwesterlies. The channelling of wind flow through a gap and across high ridges shoreward that are oblique to westerly winds could create bands of lee vortices, similar to those at L'Anse-au-Claire, which appear to be responsible for the wave forests at Ship Cove.

The Birchy Lake wave forest is little more than a decade old and therefore provides a rare opportunity to monitor the initiation and development of a wave forest. It began with a series of patches about 200 m apart on the upper slopes of a steep hill. The dead tree strips confined to the eastern side of gaps (Fig. 10(b)) are moving eastward at the rate of 15-20 m year<sup>-1</sup>. This suggests that they are the product of persistent spatial and temporal patterns of lee vortices generated by strong westerly wind intercepted at an oblique angle. This is similar to the process that shapes the wave krummholz at L'Anse-au-Claire.

Naturally, wind flow involves many processes, some of which may have a greater physical impact on forest growth than the force of wind per se. Very windy days during early and late winter are undoubtedly the most stressful time of the year for conifers. This includes the spatial and temporal distribution of freezing rain, deposition of sea salts and surfactants, abrasive ice crystals, and snow melt, as well as sub-surface biophysical processes such as soil energy fluxes, particularly patterns of soil freezing and thawing.

#### **5.4. Bifurcating forests**

The longevity of a wave forest complex is uncertain. However, the wave forests of Mt. Shimagare indicates they can persist for centuries (Oshima *et al.*, 1958). The Spirit Cove wave forest and perhaps the wave krummholz at L'Anse-au-Claire are at least 100—200 years old. A rapidly increasing number of wave forests across Newfoundland, both natural and human caused, suggests they are a relatively new

phenomenon in the Province. However, some wave forest complexes have persisted for centuries and perhaps millennia. The real issue here is what recent and perhaps unique changes, or 'oscillations', have occurred in the weather patterns that would cause an increase in the incidence of wave forests: bearing in mind that most of the coniferous forests in Newfoundland are continually being disturbed by weather and humans and apparently have rarely produced wave forest patterns until very recently.

Regardless of the causal circumstances of wave forests, they are a classic case of 'sensitive dependence on initial conditions', where slight differences between two points (events) results in substantially different outcomes. In this case, a steady-state forest responds to perturbations while more or less retaining its homogeneity. However, a bifurcation arose when an additional or a unique set of endemic disturbances occurred which led to the transformation from a steady-state forest to an unstable wave forest. The epidemic of wave forests throughout Newfoundland suggests there may have been a significant shift in the trajectories of particular types of weather systems over the region.

If that has a familiar ring of chaos to it, it should. Dynamicists refer to this process as symmetry-breaking, i.e. the onset of chaos. And what follows a wave forest complex is at issue, and much more intriguing, because it falls within that enigmatic realm of transient dynamics. Is the wave forest merely a temporary element—a kind of Hopf bifurcation (analogous to a sneeze that sends convulsions through the body)—which will eventually, over centuries, revert to a steady-state forest? Or is it a succession towards krummholz and worse? The answer lies in the non-linear dynamics of the winds, but finding the answer is a formidable challenge. The task, however, will be made a little easier by the new paradigms of circular statistics, fractal geometry and chaos theory. Also, although some progress has been made in linking a few

directional variates and fractal properties, there is still much more work to be done to integrate chaotic dynamics into reasonable holistic equations of interscale relationships in wind—forest interactions.

## **6. CONCLUSIONS**

Circular and spherical statistical algorithms are effective and efficient tools for analysing directional relationships between circular biotic variates, namely wind and processes entrained by wind, and biotic variates, such as asymmetries in growth responses of trees and forests. Theoretical distributions for both circular and spherical variates have been worked out in recent years which provide a formal test of directionality of univariate and bivariate cases. Although current models are appropriate for some types of multimodality, such as axial, triaxial and quadriaxial cases, there is no test powerful enough to distinguish between (say) a quasi-quadriaxial distribution and isotropy (random distribution). However, for almost all practical purposes this is not a major drawback. In regions dominated by unstable weather systems, circular statistics indicates that wind direction and to some extent wind speed are the only climate signals that can be detected in time series from tree rings. Circular statistics also distinguishes a phase change from biotic (competition) to abiotic (wind) as the dominant factor influencing crown asymmetry.

Fractal-based models have the potential to resolve many biometeorological problems that cannot be resolved entirely by Euclidean dimensionality. This includes a suite of fractal dimensions and topologically related chaos algorithms which resolve scaling factors and lacunarity in wind-shaped forests. Modelling wind-shaped forests as deterministic fractals requires only a few rules to decode the fractal order. Applying this principle in contraction mappings or set point topology, i.e. compressing the fractal to a point, the iterative function system (IFS) makes it possible to describe and simulate the multifractal characteristics of a wind-shaped wave forest.

There is an intense philosophical debate on the evidence for chaos. Nevertheless, as it is usually understood by physicists and meteorologists, the concept of ‘patterned instability’ is appropriate for tackling the problems of non-linear interactions between wind and forests, as so many of the processes lie within the realm of non-linear dynamics. If a natural analogue of chaos exists beyond the laboratory it is surely the wave forest phenomenon. Wave forest dynamics are patterned instabilities that are most probably created under the influence of other patterned instabilities, namely longitudinal helical roll vortices which have structural affinity to the family of Taylor vortices, and lee vortices. The wave forest phenomenon is viewed as a chaotic region within a generally stable ecosystem. The rapidly increasing incidence of wave forests appears to result from a shift in regional storm tracks. However, these relationships cannot be quantified relying solely on conventional terrestrial-based biometeorological instrumentation as the principle source of data (because it is financially, technically and logistically impractical to do so), nor on classical methods of statistical analyses and Euclidean geometry.

Applying the new paradigms of circular statistics, fractal geometry and chaos theory in conjunction with conventional approaches to quantifying the main biometeorological processes that create wave forests is of considerable importance to an understanding of interscale relationships between atmosphere and forests.

## REFERENCES

- Allen, J., 1992. Trees and their response to wind: mid Flandrian strong winds, Severn Estuary and inner Bristol Channel, southwest Britain. *Philos. Trans. R. Soc. London, Ser. B*, 338: 335-364.
- Barnsley, M., 1988. *Fractals Everywhere*. Academic Press, Boston, 394 pp.
- Barnsley, M., 1989. Lecture notes on iterated function systems. In: R. Devaney and L. Keen (Editors), *Chaos and Fractals. Proc. Symp. in Applied Mathematics. Vol. 39. American Mathematical Society, Providence, RI*, pp. 127-144.
- Batschelet, E., 1981. *Circular Statistics in Biology*. Academic Press, London, 371 pp.
- Berliner, L.M., 1992. Statistics, probability and chaos. *Statist. Sci.*, 7(1): 69-122.
- Bingham, C., 1974. An antipodally symmetric distribution on the sphere. *Ann. Statist.*, 2: 1201-1225.
- Bingham, C. and Mardia, K., 1978. A small-circle distribution on a sphere. *Biometrika*, 65: 379-389.
- Biasing, T., Solomon, A. and Duvick, D., 1984. Response curves revisited. *Tree Ring Bull.*, 44: 1-15.
- Burroughs, W., 1992. *Weather Cycles: Real or Imaginary*. Cambridge University Press, Cambridge.
- Chattargee, S. and Yilmaz, M., 1992. Chaos, fractals and statistics. *Statist. Sci.*, 7(1): 49-121.
- Chen, S., Impens, I., Ceulmans, R. and Kockelbergh, F., 1993. Measurement of gap fraction of generated canopies using digitalized image analysis. *Agric. For. Meteorol.*, 65: 245-259.
- Field, M. and Golubitsky, M., 1992. *Symmetry in Chaos*. Oxford University Press, Oxford, 218 pp.
- Fisher, R., 1953. Dispersion on a sphere. *Proc. R. Soc. London, Ser. A*, 217: 295-305.
- Fisher, N., 1993. *Statistical Analysis of Circular Data*. Cambridge University Press, Cambridge.
- Fisher, N. and Powell, C.McA., 1989. Statistical analysis of two-dimensional palaeocurrent data: methods and examples. *Aust. J. Earth Sci.*, 36: 91-107.
- Fisher, N., Lewis, T. and Embleton, B., 1987. *Statistical Analysis of Spherical Data*. Cambridge University Press, Cambridge.
- Gaines, S. and Denny, M., 1993. The largest, smallest, highest, lowest, longest, and shortest: extremes in ecology. *Ecology*, 74(6): 1677-1692.
- Grassberger, P. and Procaccia, I., 1983. Measuring the strangeness of strange attractors. *Physica*, 9D: 89-206.
- Grebogi, C., McDonald, S., Ott, E. and Yorke, J., 1985. Exterior dimension of fat fractals. *Phys. Lett. A*, 110(1): 1-4.
- Green, D., 1991. Chaos, fractals and nonlinear dynamics in evolution and phylogeny. *TREE*, 6(10): 333-337.
- Gumbel, E.J., 1958. *Statistics of Extremes*. Columbia University Press, New York.
- Hastings, H. and Sugihara, G., 1993. *Fractals: a Users Guide for the Natural Sciences*. Oxford University Press, Oxford.
- Hausdorff, F., 1919. Dimension und auusseres Mass. *Math. Ann.*, 79: 157-179.
- Holling, C., 1992. Cross-scale morphology, geometry, and dynamics of ecosystems. *Ecol. Monogr.*, 62(4):447-502.
- Hotelling, H., 1931. The generalization of Student's ratio. *Ann. Math. Statist.*, 2: 360-378.
- Jupp, P. and Mardia, K., 1980. A general correlation coefficient for directional data and related regression problems. *Biometrika*, 67: 163-173.
- Kent, J., 1982. The Fisher—Bingham distribution on a sphere. *J. R. Statist. Soc., Ser. B*, 44: 71-80.
- Korn, R., 1993. Heterogeneous growth of plant tissues. *Bot. J. Linn. Soc.*, 112: 351-371.
- Lorenz, E.N., 1963. Deterministic non-periodic flow. *J. Atmos. Sci.*, 20: 130-141.
- Mandelbrot, B., 1983. *The Fractal Geometry of Nature*. W.H. Freeman, New York, 466 pp.
- Mardia, K., 1972. *Statistics of Directional Data*. Academic Press, London, 357 pp.
- Mardia, K., 1975. Statistics of directional data. *J. R. Statist. Soc., Ser. B*, 37: 349-393.
- Mardia, K. and Spurr, B., 1973. Multisample tests for unimodal and axial circular populations. *J. R. Statist. Soc., Ser. B*, 35: 422-436.

- May, R., 1976. Simple mathematical models with very complicated dynamics. *Nature*, 261: 459-467.
- Milne, B., 1991. Lessons from applying fractal models to landscape patterns. In: M. Turner and R. Gardiner (Editors), *Quantitative Methods in Landscape Ecology*. Springer, Berlin.
- Moore, F., 1980. A modification of the Rayleigh test for vector data. *Biometrika*, 67: 175-180.
- Muircheartaigh, I. and Sheil, J., 1983. Fore or five?—the indexing of a golf course. *Appl. Statist.*, 32(3): 287-292.
- Mullin, T. (Editor), 1993. *The Nature of Chaos*. Clarendon Press, Oxford.
- Oldham, R., 1992. Architectural models, fractals and agroforestry design. *Agric. Ecosyst. Environ.*, 41: 179-188.
- Oshima, Y., Kimura, M., Iwaki, H. and Kuroiwa, S., 1958. Ecological and physiological studies of the vegetation of Mt. Shimagare I. Preliminary survey of the vegetation of Mt. Shimagare. *Bot. Mag.*, 71: 289-300.
- Peitgen, H-O., Jurgens, H. and Saupe, D., 1992. Fractals for the Classroom. Part One: *Introduction to Fractals and Chaos*. Springer, Berlin, 450 pp.
- Peters, E., 1994. *Fractal Market Analysis: Applying Chaos Theory to Investment and Economics*. Wiley, New York.
- Potvin, C. and Roff, D., 1993. Distribution-free and robust statistical methods: viable alternatives to parametric statistics. *Ecology*, 74(6): 1617-1628.
- Read, P., 1993. Applications of chaos to meteorology and climate. In: T. Mullin (Editor), *The Nature of Chaos*. Clarendon Press, Oxford.
- Rex, K. and Malanson, P., 1990. The fractal shape of riparian forest patches. *Landscape Ecol.*, 4(4): 249-258.
- Richardson, L., 1961. The problem of contiguity: an appendix of statistics of deadly quarrels. *General Systems Yearbook*, 6: 139-187.
- Robertson, A., 1987. The centroid of tree crowns as an indicator of abiotic processes in a balsam fir wave forest. *Can. J. For. Res.*, 17(7): 746-755.
- Robertson, A., 1990. Directionality of compression wood in balsam fir wave forest trees. *Can. J. For. Res.*, 20(8): 1143-1148.
- Robertson, A., 1991. Centroid of wood density, bole eccentricity and tree ring width in relation to vector winds in a wave forest. *Can. J. For. Res.*, 21: 18-19.
- Robertson, A., 1992. Recent advances in predicting the spread of birch in response to disturbance at the landscape ecology level. In: A. Aradottir (Editor), *Disturbance Related Dynamics of Birch and Birch Dominated Ecosystems. A Nordic Symposium, Illugastadir, Fnjoskodalur, Iceland*. Iceland Forest Research Station, Mogilsa.
- Robertson, A., 1993a. Wave forests. In: J. Alden and L. Mastrandiano (Editors), *Forest Development in Cold Climates*. Plenum, New York.
- Robertson, A., 1993b. Effects of wind on northern forests. In: J. Alden and L. Mastrandiano (Editors), *Forest Development in Cold Climates*. Plenum, New York.
- Robertson, A., 1993c. Forest climate. In: A. Robertson, S. Porter and G. Brody (Editors), *Climate and Weather of Newfoundland*. Creative Publishers, St. John's, Nfld.
- Sceicz, G., Petzold, D. and Wilson, R., 1979. Wind in the subarctic forest. *J. Appl. Meteorol.*, 18: 1268-1274.
- Schertzer, D. and Lovejoy, S., 1991. Nonlinear geodynamical variability: multiple singularities, universality and observables. In: D. Schertzer and S. Lovejoy (Editors), *Scaling, Fractals and Non-linear Variability in Geophysics*. Kluwer, Dordrecht.
- Scott, P., Fayle, D., Bentley, C. and Hansell, R., 1988. Large-scale changes in atmospheric circulation interpreted from patterns of tree growth at Churchill, Manitoba, Canada. *Arct. Alp. Res.*, 29(2): 199-211.
- Selby, B., 1964. Girdle distribution on a sphere. *Biometrika*, 51: 381-392.
- Smith, R., 1991. Comment: relation between statistics and chaos. *Statist. Sci.*, 7(1): 109-113.
- Stewart, I., 1992. *The Problems of Mathematics*. Oxford University Press, Oxford.

- Sugihara, G., Grenfell, B. and May, R., 1990. Distinguishing error from chaos in ecological time series. *Philos. Trans. R. Soc. London, Ser. B*, 330(1257): 121-304.
- Takens, F., 1981. Detecting strange attractors in turbulence. In: D.A. Rand and L.S. Young (Editors), *Dynamical System and Turbulence. Lecture Notes in Mathematics*, Vol. 898. Springer, New York, pp. 366-381.
- Turner, M., Gardner, R., Dale, V. and O'Neill, R., 1989. Predicting the spread of disturbance in heterogeneous landscapes. *Oikos*, 55: 121-129.
- Upton, G. and Fingleton, B., 1989. Spatial Data Analysis by Example: Vol. 2, Categorical and Directional Data. Wiley, Chichester, 416 pp.
- Van Deusen, P., 1989. Stand dynamics and red spruce decline. *Can. J. For. Res.*, 20: 743-749.
- Vautard, R. and Ghil, M., 1989. Singular spectrum analysis in nonlinear dynamics, with applications to paleoclimatic time series. *Physica, D*, 35: 395-424.
- Wade, J. and Hewson, F., 1979. Trees as a local climate indicator. *J. Appl. Meteorol.*, 19: 1182-1187.
- Wang, X-J. and Gaspard, P., 1992. Entropy for a time series of thermal turbulence. *Phys. Rev., A*, 46(6): R3000-3003.
- Watson, G., 1965. Equatorial distributions on a sphere. *Biometrika*, 52: 193-201.
- Wolf, A., Swift, J.B., Swinney, H.L. and Vvasano, J.A., 1985. Determining Lyapunov exponents from a time series. *Physica, 16D*: 285-317.
- Wood, A., 1982. A bimodal distribution on the sphere. *Appl. Statist.*, 31: 52-58.
- Wood, E. and Lakshmi, V., 1993. Scaling water and energy fluxes in climate systems: three land— atmosphere modeling experiments. *J. Climate*, 6: 839-857.
- Yoshino, M., 1988. An international scale of wind-shaped trees as an indicator of climatic conditions. *26th Congress, International Geographical Union, Sydney, Australia, 21-26 August 1988*.
- Zak, J. and Minnich, R., 1991. Integration of geographic information systems with a diagnostic wind field model for fire management. *For. Sci.*, 37(2): 560-573.
- Zar, J., 1974. Biostatistical Analysis. Prentice—Hall, Englewood Cliffs, NJ.
- Zeide, B., 1993. Primary unit of the tree crown. *Ecology*, 74: 1598-1602.
- Zeide, B. and Gresham, C., 1991. Fractal dimensions of tree crowns in three loblolly pine plantations of coastal South Carolina. *Can. J. For. Res.*, 21: 1208-1212.
- Zeide, B. and Pfeifer, P., 1991. A method for the estimation of fractal dimension of tree crowns. *For. Sci.*, 37(5): 1253-1265.